# The Effect of Temperature on the PZT Sensor Response—Case Study with Guided Wave SHM

BENGISU YILMAZ, ARNAUD RECOQUILLAY
and BASTIEN CHAPUIS

**ABSTRACT**

The guided wave structural health monitoring (GWSHM) systems can provide continuous monitoring of the critical engineering structures in several industries including energy and aerospace. Today's digital tools, like numerical simulations, can provide rapid and extensive knowledge about GWSHM systems without the cost of implementation. On the other hand, the effect of environmental factors like temperature plays an important role in the GWSHM system response. To fully simulate the system, it is then mandatory to have reliable models for these factors. To this date, several research groups conducted studies to understand the effect of temperature variances on material properties; however, there is a lack of fast models for sensor response.

This work focuses on the generalization of the pin-force PZT response model available in the software CIVA under varying temperatures (typ. from -20°C to 40°C). Measured impedance values were used to estimate the effective radius of the bonded PZTs. The numerical studies were validated experimentally on a case study without damage. By using proposed technique, the effect of temperature on the sensor definition, including bonding, is implemented in the numerical studies. Furthermore, this is an important step towards model assisted probability detection (MAPOD) of the systems under different environmental conditions.

Bengisu Yilmaz, University of Paris Saclay, CEA List, F-91120 Palaiseau, France
Arnaud Recoquillay, University of Paris Saclay, CEA List, F-91120 Palaiseau, France
Bastien Chapuis, University of Paris Saclay, CEA List, F-91120 Palaiseau, France

## INTRODUCTION

Guided wave Structural Health Monitoring has been a subject of interest over the years for its capability to monitor large structures using a limited number of sensors. In this context, piezoelectric patches have been widely studied [1] due to their ability to emit and receive ultrasonic waves while having a limited intrusiveness.
A key component nowadays to design and qualify such a system is simulation. Indeed, as the system may encounter a wide variety of environmental and operational conditions, a large number of cases need to be considered in these phases. Hence the need for fast and reliable simulations to limit the time needed for such studies. Among the influencing environmental parameters, temperature variation has been widely studied due to its large effect on guided wave signals and its common occurrence in applications. This parameter influences wave propagation [3] as well as sensor responses [11].
Regarding the sensors in particular, one possibility is to fully model the piezoelectric effect occurring inside the sensor when all the corresponding parameters are available and at a potentially large computational cost [13]. Several simplified models have been developed to efficiently simulate the actuation and response of piezoelectric patches to guided waves with a limited number of parameters. The most famous model is the Pin Force model [5], enabling to model the sensor by a simple load along its edge, needing only the knowledge of the radius of the sensor, under the assumption of an infinitely thin coupling medium. It has been further refined in particular thanks to the Shear-Lag model [6] to take into account the coupling medium, needing to characterize it. Other approaches exploiting empirical parameters have also been studied to limit the needed knowledge over potentially hard to obtain parameters to fully characterize the sensor as well as the coupling medium [8][7]. An easy to access empirical parameter of the sensor is the electromechanical impedance, which has been used to calibrate the Shear-Lag model [4].
The aim of this study is to use electromechanical impedance measured at different temperatures to improve the accuracy of simulations with respect to temperature variations. The first part is dedicated to the introduction of the used models and the second part to a comparison to experimental results.

## MODEL DESCRIPTION

### Wave propagation model

The simulations are performed using the SHM module of CIVA, which solves fully three-dimensional elastic problems in the time domain. It relies on a parametric description of the structure and its features, enabling the use of unassembled spectral finite elements in space and a leapfrog scheme in time. By doing so, low memory consumption and fast computations are achieved, suited for large parametric studies [10]. For more details, the interested reader can refer to [9]. The input material parameters are Hooke's tensor and mass density. It is well known that Hooke's tensor, which can be summarized by the knowledge of wave velocities and mass density in an isotropic medium, is mainly affected by temperature variations. These variations can hence be taken into account by modifying these values. In this study, we considered only a linear dependency with respect to temperature as can be found in [2].

**Sensor model**

Due to its simplicity and low computational cost, the Pin-Force model is used in CIVA to approximate classic circular piezoelectric patches. A unitary load normal to the radius of the sensor is prescribed by the model. As we are considering here finite elements in space, we need to define a surface over which the load is applied. An annulus is hence defined at the edge of the sensor through the definition of an inner and an outer radius. The width of this annulus is taken as a trade-off between computation time, as reducing too much this width would imply badly shaped mesh elements and higher computation times, and the fidelity to the original model, which corresponds to a null width. A specific mesh pattern is defined to enable this definition.

As mentioned in the introduction, a Shear-Lag model can be easily calibrated through the measurement of electromechanical impedances [4], giving the effective area of the sensor through:

$$A_{effective} = \left| \frac{Y_{bonded}}{Y_{free}} \right| A_{nominal},$$

Where $Y_{bonded}$ and $Y_{free}$ are respectively the electromechanical admittance of the bonded and free sensor, and $A_{effective}$ and $A_{nominal}$ are respectively the effective and nominal area. These impedances depend on the frequency. For our time solver, we considered only the values at the center frequency. Note also that, as the sensors may have resonant behaviors in the vicinity of the frequency of interest, the used impedances are obtained through a linear fit of the impedance with respect to frequency [4]. These two impedance measurements can easily be done at various temperatures.

## COMPARISON TO EXPERIMENTAL DATA

**Description of the experimental use case**

A square 3 mm thick aluminum panel of side length 600 mm is considered. Longitudinal and shear wave velocity were measured using bulk waves at ambient temperature. The obtained values are respectively 6482 $\mathrm{m.s^{-1}}$ and 3131 $\mathrm{m.s^{-1}}$. Two 12 mm diameter sensors from Steminc PI (SMD12) have been glued using epoxy 300 mm apart on the plate along the diagonal, the first sensor being respectively 240 mm and 200 mm from adjacent sides.

A climate chamber is used to perform experiments at temperatures ranging from -10°C to 40°C by 5°C steps. A waiting time of 90 minutes was observed between temperature stabilization of the climate chamber and measurements at each step to ensure a homogeneous temperature. Electromechanical impedances of the sensors were acquired before and after bonding using an impedance analyzer over then range 20 Hz to 800 kHz. Regarding the ultrasonic guided wave data, the first sensor was actuated using an arbitrary waveform generator with an amplitude of 9.5 Vpp. The data were recorded using a preamplifier with an order 2 high-pass filter of cutoff frequency 10 kHz and a gain of 2 before digitization by an oscilloscope. Data were averaged 600 times to limit Two source signals were considered, which were 4 cycle Hann burst of center frequency 50 kHz and 80 kHz.

**Description of the model parameters**

The geometrical parameters were inputted in the software. The evolution of the material parameters with respect to temperature was described according to [2]:

$$c_L(T) = c_L(T_0) - \ (1.47 * (T - T_0))$$
$$c_S(T) = c_S(T_0) - \ \big(0.92 * (T - T_0)\big),$$

Where $c_L$ and $c_S$ are respectively the longitudinal and shear wave velocity, $T_0 = 20°C$ is the ambient temperature at which these velocities were measured using bulk waves.

Effective radii were extracted from admittance measurements. The linear fits were fitted over the range (15; 40) kHz to limit the impact of resonances occurring around 200 kHz in the free case. The corresponding measurements and linear fits are plotted in Figure 1. Note that the linear fits in the bonded case are very close to true admittance values, the resonance being shifted to higher frequencies. Admittance values are globally increasing with temperature both for bonded and unbonded sensor.

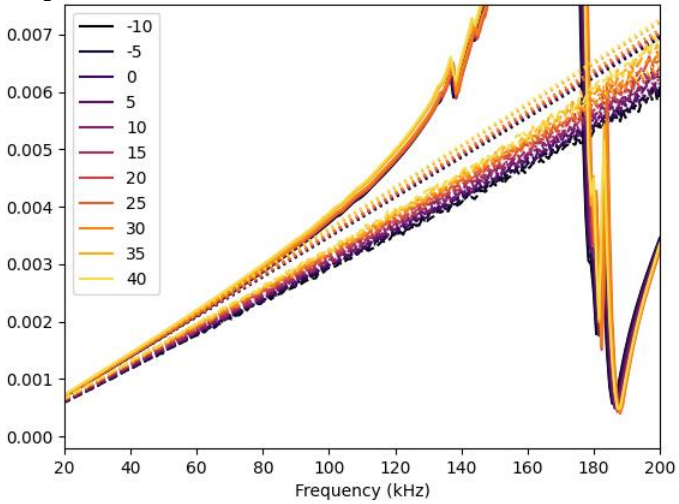


Figure 1. Admittance measurements for varying temperatures for the first sensor. Continuous lines: bonded transducers. Dashed lines: free transducers. Dotted lines: linear fits.

The excitation annulus was fixed at 1 mm, the effective radius corresponding to the average between the inner and outer radius. In other terms, we have $r_{in}(T) = r_{eff}(T) - 0.5$ and $r_{out}(T) = r_{eff}(T) + 0.5$.

For the sake of completeness, we also performed simulations when only the effect of temperature on material parameters is taken into account, the effective radius being taken as the one obtained at 20°C.

First, the case of a source of center frequency 80 kHz is considered. This frequency was chosen as it enables a good separation in time of both A0 and S0 modes with no mode being negligible. We first compared the simulated signal and the experimental one in Figure 2 left at 20°C. Note that the simulation is up to an amplitude factor, so for the sake of comparison both signals have been normalized with respect to their respective maximum. We see a very good match between the two signals, the relative amplitude of the wave packets being similar. We can also see that the edge reflection of S0, starting around 175 µs, is also rather well simulated. We also plotted in Figure 2 right the experimental signals with varying temperature, each signal corresponding to a different temperature. We can see, especially for the A0 wave packet, a change in amplitude and time of flight.

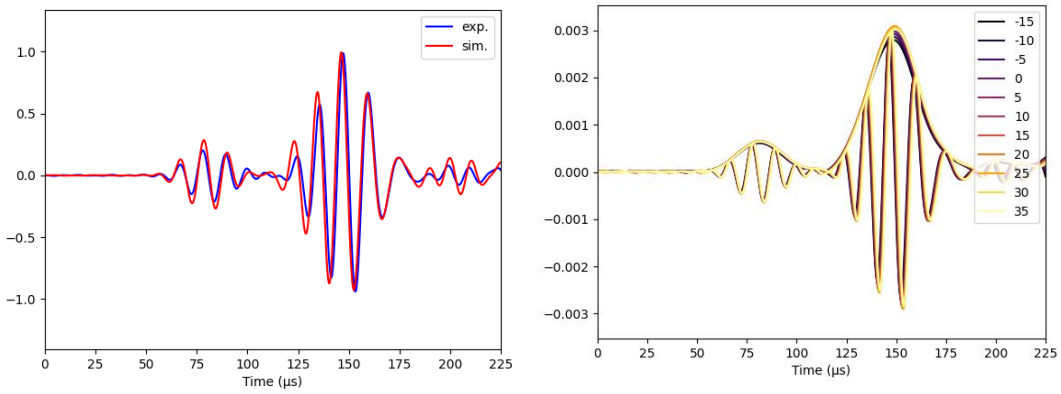


Figure 2. Signals for the 80 kHz excitation. Left: comparison between experiment and simulation. Right: evolution of experimental signals with temperature. Each color corresponds to a different temperature.

To compare simulation and experiments at different temperatures, we focalized on these two parameters for both wave packets. In Figure 3 and Figure 5, we plotted their evolutions for the experimental data, the simulated ones without temperature effect on the sensors and for the full model. More precisely, the parameters are computed as

$$\Delta t_n(T) = t_n(T) - t_n(T_0),$$

$$\Delta A_n(T) = \frac{A_n(T)}{A_n(T_0)},$$

Where $t_n(T)$ and $A_n(T)$ are respectively the time of flight and the amplitude of mode $n$ at temperature $T$.

First, regarding the time of flight in Figure 3 left, we see a very good agreement for the A0 mode between both models and the experiment. This is expected as the time of flight change comes mainly from the shift in material parameters. There is a slight difference, of the order of 0.1 µs, when adding the sensor model compared to only considering the effect on the materials. This is indeed due to the change of effective radius, which is at most of 0.15 mm between its minimum and maximum value. We have similar trends for the S0 mode but with a higher discrepancy between simulation and experiment. This may be due to a higher sensitivity of the S0 mode energy velocity to parameter changes: remember indeed that the variations of $c_L$ and $c_S$ with respect to temperature were taken from the literature. True values for our samples may differ slightly. Note that the difference is in any case less than 1 µs.

In the case of amplitude, variations in material parameters induce a small linear amplitude increase with temperature for both modes. This variation is however smaller than the one observed in experiments, which do not follow a linear trend. The addition of the effect of temperature on the sensors helps reducing the gap. There is a rather good fit for temperatures between 0°C and 20°C. Below 0°C, the discrepancy increases, in particular for the A0 mode. This may come partially from the use of a linear temperature model for material parameters, not enabling to fully take into account variations for higher temperature variations. Above 20°C, we actually see an inflexion of the amplitude change in the experiments: the amplitude starts decreasing with temperature. This phenomenon has already been observed [11][12] and may come from an increased variation in the dielectric permittivity $e_{33}$ compared to the piezoelectric coefficient $d_{31}$. This effect may differ depending on the exact material of the used transducers, but both the used sensors and the ones from [11][12] are in PZT 5A. The inflexion point is also obtained in simulations, but for higher temperatures.

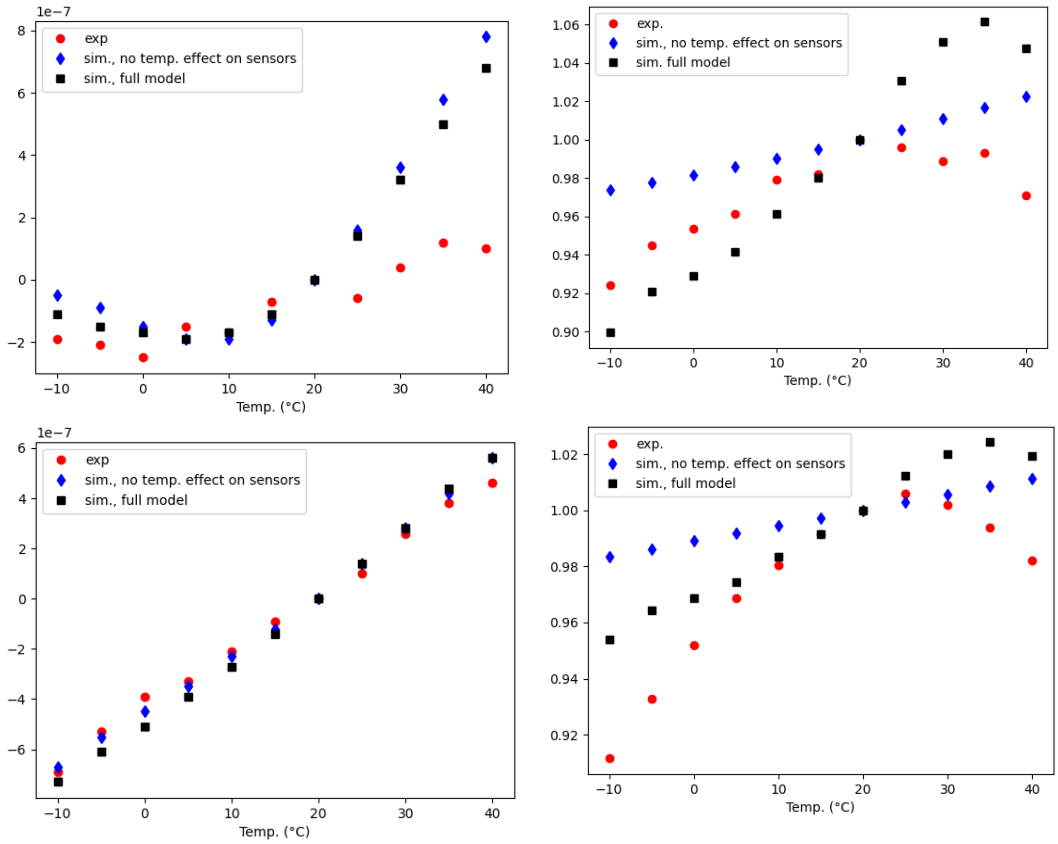


Figure 3. Evolution of wave packet parameters with respect to temperature for the 80 kHz excitation. Left: Time of Flight shift. Right: amplitude shift. Top: S0 mode. Bottom: A0 mode.

The same study was done for the excitation signal of center frequency 50 kHz. Similar results are obtained for the comparison between simulation and experiment (Figure 4 left) and variation with temperature of experimental signals (Figure 4 right). The main differences are that the amplitude ratio between S0 and A0 mode is significantly lower, and the first S0 wave packet is composed of the direct wave packet as well as edge reflections, which can be seen from the shape of the packet.

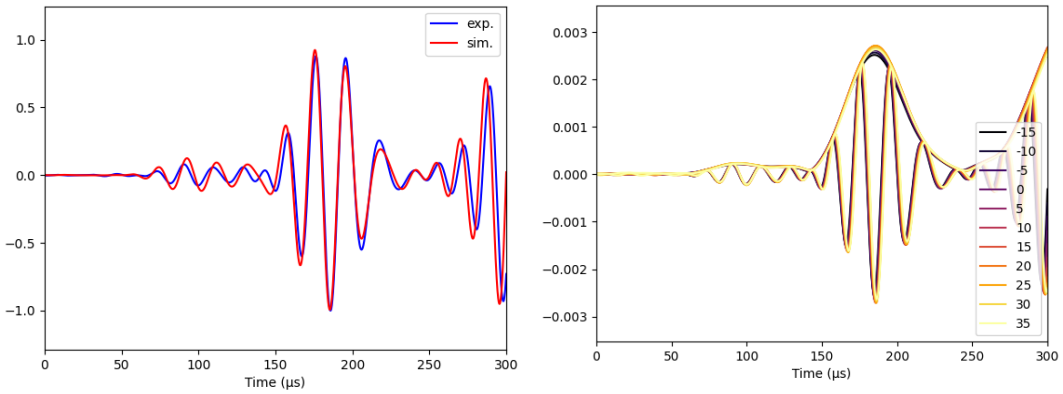


Figure 4. Signals for the 50 kHz excitation. Left: comparison between experiment and simulation. Right: evolution of experimental signals with temperature. Each color corresponds to a different temperature.

Regarding the wave packet characteristics, in Figure 5, the same behaviors as before are observed for the A0 mode. For the S0 mode, the extraction is noisier in the experimental data, due to the interaction with edge reflections. In particular, values extracted at 20°C,

which are used to calibrate the curves, are lower than expected, leading to shifts in the obtained experimental curves. For the sake of completeness, the same parameters with $T_0 = 15°C$ have been added in Figure 6.

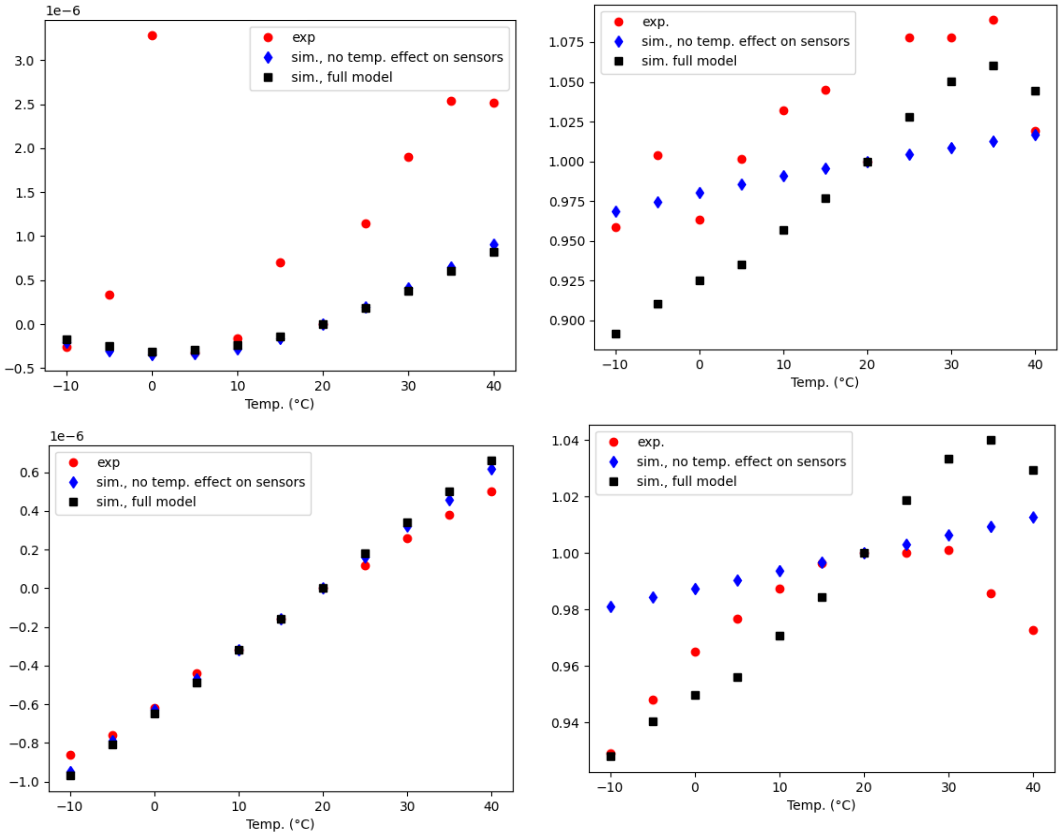


Figure 5. Evolution of wave packet parameters with respect to temperature for the 50 kHz excitation. Left: Time of Flight shift. Right: amplitude shift. Top: S0 mode. Bottom: A0 mode.

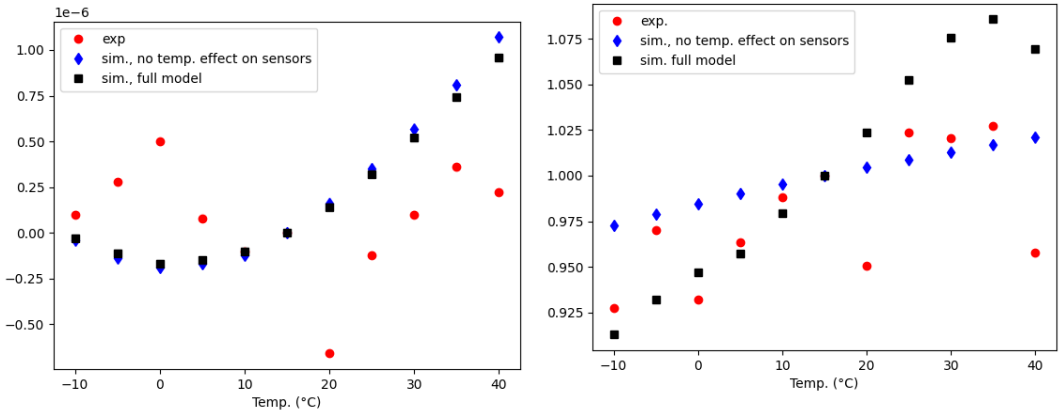


Figure 6. Evolution of S0 mode parameters with respect to temperature for the 50 kHz excitation and 15°C as reference temperature. Left: Time of Flight shift. Right: amplitude shift.

## CONCLUSION

This study focused on the use of admittance measurements to calibrate the shear-lag model in a varying temperature environment. It shows that it enables to reduce the gap between simulation and experiment while not changing the computational burden. As already remarked in [4], the main advantage of such an approach is the need only of free and bonded admittance measurements, which are rather easy to obtain. Further refinement may be needed for high temperatures, for which the signal amplitude decrease is not well retrieved in simulations.

## REFERENCES


[1] M. Mitra, and S. Gopalakrishnan. Guided wave based structural health monitoring: A review. *Smart Materials and Structures*, 2016, vol. 25, no 5, p. 053001.

[2] E. Ginzel and R. Ginzel, "Approximate dV/dT values for some materials". *e-Journal of Nondestructive Testing*, 2017, https://www.ndt.net/?id=21545

[3] T. Clarke, F. Simonetti, and P. Cawley. Guided wave health monitoring of complex structures by sparse array systems: Influence of temperature changes on performance. *Journal of Sound and Vibration*, 2010, vol. 329, no 12, p. 2306-2322.

[4] H. Sohn and S. J. Lee, "Lamb wave tuning curve calibration for surface-bonded piezoelectric transducers," *Smart Mater. Struct.*, vol. 19, no. 1, p. 015007, Jan. 2010, doi: 10.1088/0964-1726/19/1/015007.

[5] V. Giurgiutiu. Tuned Lamb wave excitation and detection with piezoelectric wafer active sensors for structural health monitoring. *Journal of intelligent material systems and structures*, 2005, vol. 16, no 4, p. 291-305.

[6] E. Crawley, and E. Anderson. Detailed models of piezoceramic actuation of beams. *Journal of Intelligent Material Systems and Structures*, 1990, vol. 1, no 1, p. 4-25.

[7] S. Sharma, O. Mesnil, A. Recoquillay, *et al.* A Hybrid Actuator Model for Efficient Guided Wave-Based Structural Health Monitoring Simulations. *Journal of Nondestructive Evaluation, Diagnostics and Prognostics of Engineering Systems*, 2024, vol. 7, no 4, p. 041005.

[8] N. Quaegebeur, P. Ostiguy, and P. Masson. Hybrid empirical/analytical modeling of guided wave generation by circular piezoceramics. *Smart Materials and Structures*, 2015, vol. 24, no 3, p. 035003.

[9] O. Mesnil, A. Recoquillay, T. Druet, *et al.* Experimental validation of transient spectral finite element simulation tools dedicated to guided wave-based structural health monitoring. *Journal of Nondestructive Evaluation, Diagnostics and Prognostics of Engineering Systems*, 2021, vol. 4, no 4, p. 041003.

[10] B. Yilmaz, S. Sharma, A. Recoquillay, *et al.* A model assisted probability of detection for guided wave SHM systems: comparative study on recent statistical developments. *e-Journal of Nondestructive Testing*, 2024, https://www.ndt.net/?id=29839

[11] F. Lanza Di Scalea, and S. Salamone. Temperature effects in ultrasonic Lamb wave structural health monitoring systems. *The Journal of the Acoustical Society of America*, 2008, vol. 124, no 1, p. 161-174.

[12] H.-J. Lee and D. Saravanos. The effect of temperature dependent material properties on the response of piezoelectric composite materials. *Journal of intelligent material systems and structures*, 1998, vol. 9, no 7, p. 503-508.

[13] C. Bellis and S. Impériale. Reciprocity identities for quasi-static piezoelectric transducer models: Application to cavity identification using iterated excitations and a topological sensitivity approach. *Wave Motion*, 2014, vol. 51, no 1, p. 125-145.